FINNISH CARDIAC SOCIETY

52nd Progress Report Meeting

April 15, 2026, Helsinki

Contents

52nd Progress Report Meeting Programme

Bysa 3, Session 1. 52nd Progress Report Meeting – Young Investigators Award Competition

Chairperson Erkki Ilveskoski, Tampere Heart Hospital

Meeting is supported by unrestricted educational grant from Boehringer Ingelheim

10.00–10.05	Video by Progress Report Competition supporter Boehringer Ingelheim.
10.05–10.10	Opening remarks. Chairperson Erkki Ilveskoski, Tampere Heart Hospital
10.10–10.20	From hypertension to heart failure with preserved ejection fraction – optimisation and characterisation of clinically relevant mouse model. Diana Törmä, Master of Science, A.I. Virtanen Institute, University of Eastern Finland
10.20–10.30	Evolution and echocardiographic follow-up of mild and moderate primary mitral valve regurgitation. Miikka Surakka, MD, Heart Center, Turku University Hospital
10.30–10.40	Rotating frame spin-lock cardiac magnetic resonance imaging method can distinguish diffuse myocardial fibrosis in heart failure with preserved ejection fraction in mice at 9.4 T. Riku Kiviluoto, MSc, University of Eastern Finland
10.40–10.50	Does the association between oral anticoagulation and stroke risk differ by CHA_2DS_2-VA score in patients with atrial fibrillation? A nationwide cohort study. Eero Jalli, MD, Satasairaala
10.50–11.00	Next-generation sudden cardiac death risk assessment in hypertrophic cardiomyopathy: integrating cardiac magnetic resonance imaging with artificial intelligence. Lotta Poltto, Master of Science, HUS Helsinki University Hospital
11.00–11.10	Combined targeting of AT1 and CTGF for heart failure therapy. Samu Saarimäki, Master of Science, University of Oulu
11.10–11.20	A Deep Neural Network for Interpreting Wearable ECG Data in Atrial Fibrillation. Olli Rantula, MD, MSc, University of Eastern Finland
11.20–11.30	The presence of cysts suggests for degenerative acute type A aortic dissection. Essi Pirskanen, Medical Student, Tampere University Heart Hospital and Tampere University
11.30–11.40	Non-invasive imaging of the sinoatrial node structure using quantitative MRI: from histology-validated ex vivo porcine study to first human in vivo assessment. Yi Li, PhD Candidate, University of Oulu
11.40–11.50	Association between aortic length and 4D flow parameters: wall shear stress and flow displacement. Ansa Hakala, Bachelor of Medicine, University of Eastern Finland
11.50–11.55	Closing remarks.

History of the Progress Report Meetings

Progress Report Meeting is organized by Finnish Cardiac Society to present opportunity for young investigators to report results of their studies. An important point is also training in presenting scientific papers to criticism of senior colleagues.
Boehringer Ingelheim has supported organizing the meeting from the beginning, 1975 by helping in practical matters and presenting grants to the best of speakers.

Winners of the Boehringer Ingelheim grants

From year 2007 onwards the competition has had two categories (basic science and clinical research) instead of 1st and 2nd prize. In 2021 rules were changed so that upon the decision of the judges, the categories can be combined (if less than three eligible abstracts have been received to either category); both categories will have 1st place or there will be 1st and 2nd place when categories are combined.

Year	1st Prize	2nd Prize
1975	Erkki Pesonen	--
1976	Heikki Karppanen	Markku S. Nieminen
1977	Matti Halinen	Ulla Korhonen
1978	Ilkka Torstila	Markku S. Nieminen
1979	Olli Meretoja	Aila Rissanen
1980	Jorma Viikari	Jouko Jalonen
1981	Markku Kupari	Irma Koivula
1982	Heikki Huikuri	Markku Kupari
1983	Seppo Hietakorpi	Kari Niemelä
1984	Markku Laakso	Heikki Huikuri
1985	Jukka Räisänen	Kari Niemelä
1986	Pekka Koskinen	Juha Mustonen
1987	Kimmo Mattila	Silja Majahalme
1988	Heikki Tikkanen	Paula Rämö
1989	Hannu Näveri	Keijo Peuhkurinen
1990	Markku Mäkijärvi	Juhani Valkama
1991	Eero Mervaala	Paavo Uusimaa
1992	Eero Mervaala	Anne Remes
1993	Juha Hartikainen	Helena Kovanen
1994	Kai Kiilavuori	Juha Perkiömäki
1995	Sirkku Pikkujämsä	Pasi Tavi
1996	Jorma Kokkonen	Timo Mäkikallio
1997	Pekka Raatikainen	Marja Laitinen
1998	Marja Laitinen	Antti Ylitalo, 3rd Prize Timo Mäkikallio
1999	Mika Laine	Timo Mäkikallio
2000	Saila Vikman	Antti Kivelä
2001	Jari Tapanainen	Pertti Jääskeläinen
2002	Tuomas Rissanen	Markku Pentikäinen
2003	Juhani Junttila	Markus Leskinen
2004	Jere Paavola	Tuomas Rissanen
2005	Mikko Mäyränpää	Satu Helske
2006	Olli Tenhunen	Johan Lassus
Year	**Basic Science category**	**Clinical Research category**
2007	Satu Helske	Ville Kytö
2008	Mirella Hietaniemi	Minna Kylmälä
2009	Johanna Lähteenvuo o.s. Markkanen	Annukka Marjamaa
2010	1st Prize Jani Tikkanen 2nd Prize Riina Kandolin	the categories were combined
2011	Markku Lähteenvuo	Aapo Aro
2012	1st Prize Kirsi Kujala 2nd Prize Maija Bry	the categories were combined
2013	Suvi Syväranta	Toni Grönberg
2014	1st Prize Leena Kaikkonen 2nd Prize Heli Tolppanen	the categories were combined
2015	1st Prize Aissa Bah 1st Prize Markus Räsänen	the categories were combined
2016	1st Prize Heli Tolppanen 1st Prize Kaj Ekström	the categories were combined
2017	Tarja Alakoski	Samuli Jaakkola
2018	Maija Ruuth	Tero Penttilä
2019	Annakaisa Tirronen	Anette Haukilahti
2020	1st Prize, Tiia Istolahti 1st Prize, Henna Korpela 2nd Prize, Vilbert Sikorski	the categories were combined
2021	1st Prize Aleksi Leikas 2nd Prize Minna Koivunen	the categories were combined
2022	1st Prize Markus Ritvos 2nd Prize Kristiina Harju	the categories were combined
2023	1st Prize Anne Doedens 2nd Prize Valtteri Muroke	the categories were combined
2024	1st Prize Marko Taipale 2nd Prize Lauri Äikäs	the categories were combined
2025	1st Prize Erika Atencio Herre 2nd Prize Henri Kesti	the categories were combined

Presentation time
10.10-10.20

Diana Törmä, Master of Science
A.I. Virtanen Institute, University of Eastern Finland

From hypertension to heart failure with preserved ejection fraction – optimisation and characterisation of clinically relevant mouse model

Diana Törmä, A.I. Virtanen Institute, University of Eastern Finland; Tuisku Suoranta, A.I. Virtanen Institute, University of Eastern Finland; Mimmi Rinta-Harri, A.I. Virtanen Institute, University of Eastern Finland; Anna-Kaisa Ruotsalainen, A.I. Virtanen Institute, University of Eastern Finland; Seppo Ylä-Herttuala, A.I. Virtanen Institute, University of Eastern Finland

Aim

Heart failure with preserved ejection fraction (HFpEF) is a complex syndrome characterised by systemic low-grade inflammation, endothelial dysfunction and extracellular matrix rearrangement that lead to diastolic impairment and permanently altered cardiac architecture and dynamics. Diagnosis of HFpEF is challenging due to heterogenous disease aetiology and asymptomatic early stages. This highlights the need for the adequate HFpEF and early-HFpEF animal models that will help better understand underlying disease mechanisms, provide insight into initial phases of HFpEF, help develop and test HFpEF-targeted therapeutics and improve diagnostic approaches.

Methods

Phenotype was induced in C57BL/6JOlaHsd male mice with angiotensin II (Ang II)-infused s.c. implanted osmotic minipumps for 28 days. For gradual progression of hypertensive HFpEF progression in mice, we used two separate approaches: 1) longitudinal advancement of the phenotype with several timepoints and 2) dose-dependent syndrome progression with four different doses (0.5 – 2.4. mg/kg/day) of Ang II infusions. To provide detailed characterisation of HFpEF stages, clinically relevant imaging methods and parameters were used. Murine transthoracic echocardiography, cardiac magnetic resonance imaging (cMRI), ECG monitoring and blood pressure measurements were performed to detect changes in cardiac contractility and visualise myocardial remodelling and its effects. Extensive histology and immunohistochemistry analyses were done to characterise myocardial modifications and identify early pathological changes. To estimate the advancement of diastolic dysfunction and myocardial stiffening, qPCR analyses were also performed.

Results

We identified two clear hypertensive heart disease phenotypes that showed similar levels of hypertension and microvascular rarefaction but different stages of myocardial hypertrophy and fibrotic remodelling, which suggested Ang II dose-dependency. Interestingly, our results revealed early structural and functional aortic modifications in the lowest Ang II dose group, demonstrating that these pathologies to occur early in disease progression, prior to diastolic impairment. Importantly, we were able to show alterations in electrical impulse propagation in affected hearts, which is rarely shown in mice. We also demonstrated systemic pathologies present in lungs and kidneys.

Conclusions

Ang II-induced hypertensive HFpEF in mice is an adequate disease model to recapitulate clinical HFpEF phenotype features, capture syndrome progression and recognise its earlier stages. This model is further utilised in studying molecular mechanisms involved in the advancement of diastolic impairment and myocardial remodelling, investigation of clinically feasible new imaging methods and, importantly, used as a platform for testing new HFpEF-specific therapeutics.

Presentation time
10.10-10.20

Diana Törmä, Master of Science
A.I. Virtanen Institute, University of Eastern Finland

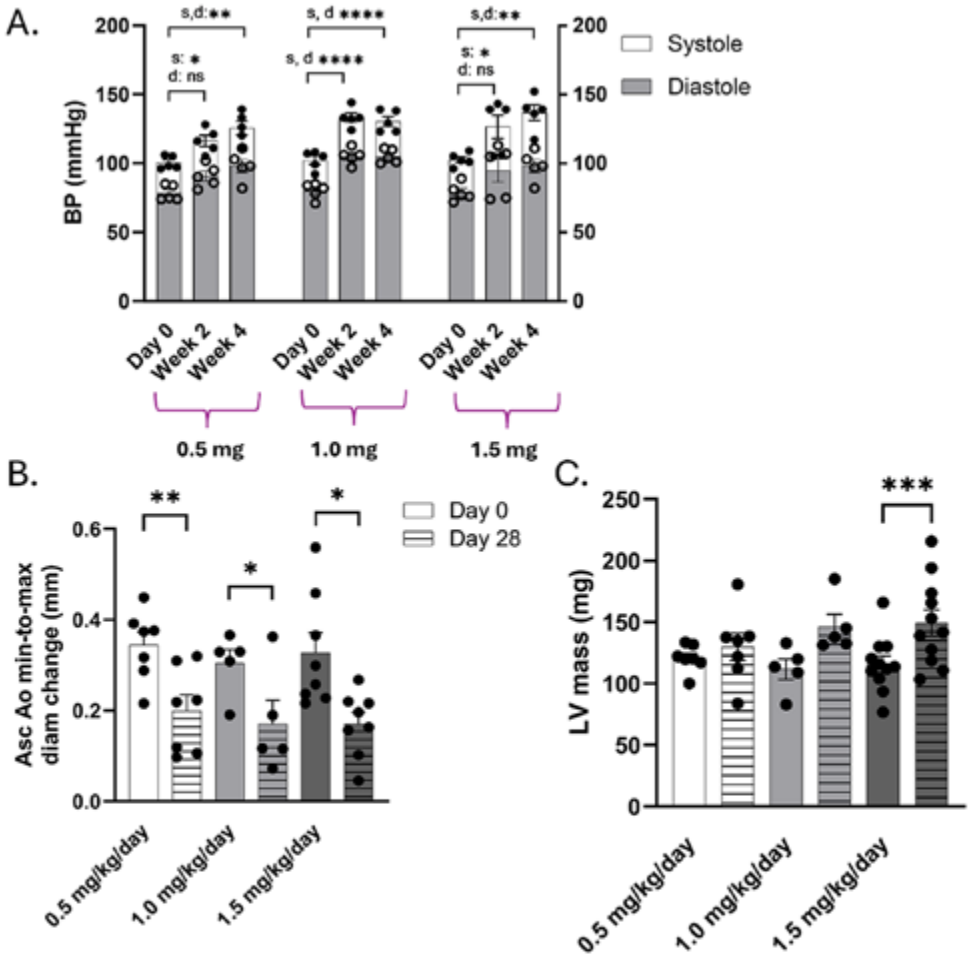

Figure 1. Levels of hypertension (A), both systolic and diastolic, were similar. Significant alterations in aortic wall dynamics (B) were present in three dose groups, preceding hypertrophy in two lowest dose groups (C). *Asc Ao, ascending aorta; BP, blood pressure; s, systole; d, diastole; LV, left ventricle; ns, not significant.*

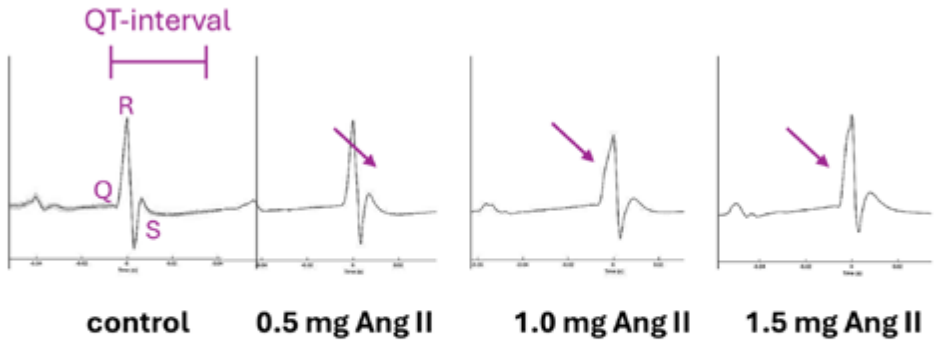

Figure 2. Significant prolongation of total ventricular depolarisation and repolarisation times (QT) in all Ang II dose groups by day 28 of the experiment.

Presentation time
10.20-10.30

Miikka Surakka, MD
Heart Center, Turku University Hospital

Evolution and echocardiographic follow-up of mild and moderate primary mitral valve regurgitation

Miikka Surakka, Heart Center, Turku University Hospital; Rosa Hirvonen, Heart Center, Turku University Hospital; Tuija Vasankari, Heart Center, Turku University Hospital; Wail Nammas, Heart Center, Turku University Hospital; Juhani Airaksinen, Heart Center, Turku University Hospital; Heikki Ukkonen, Heart Center, Turku University Hospital; Antti Saraste, Heart Center, Turku University Hospital

Aim

Serial echocardiographic follow-up of patients with mitral regurgitation (MR) is common practice and recommended by clinical practice guidelines, yet contemporary data on the natural course of primary MR, particularly in those without severe regurgitation at presentation, remain limited. We aimed to study the natural course of primary MR, particularly mild MR, during serial echocardiographic follow-up.

Methods

We retrospectively identified patients with MR who underwent serial echocardiographic follow-up between 2004-2019. Patients with secondary MR due to heart failure or concomitant severe valvular disease were excluded. Age and sex matched individuals without valvular or structural heart disease served as controls. Data on MR severity, all-cause mortality, cardiovascular events and MR interventions were collected.

Results

The study cohort comprised 613 patients with mild (n=274), moderate (n=221) or severe (n=118) MR. During a mean follow-up of 6.1±3.8 years, patients underwent an average of 4.3 echocardiographic examinations. Compared with moderate MR, fewer patients with mild MR progressed to severe MR during follow-up (3.6% vs. 27.6%, $p<0.001$). Interventions for MR occurred in 3.3% of patients with mild MR, compared with 21% and 64% of those with moderate and severe MR, respectively ($p<0.001$). Among patients with mild MR, symptoms triggered intervention in 8 out of 9 cases; all had preserved post-operative left ventricular ejection fraction. Overall survival was similar between patients with mild MR and matched controls.

Conclusions

Only a small proportion of patients with mild primary MR progress to severe MR or require surgery over approximately six years of follow-up. When intervention is required, it is predominantly symptom-driven and associated with preserved post-operative left ventricular systolic function.

Presentation time
10.20-10.30

Miikka Surakka, MD
Heart Center, Turku University Hospital

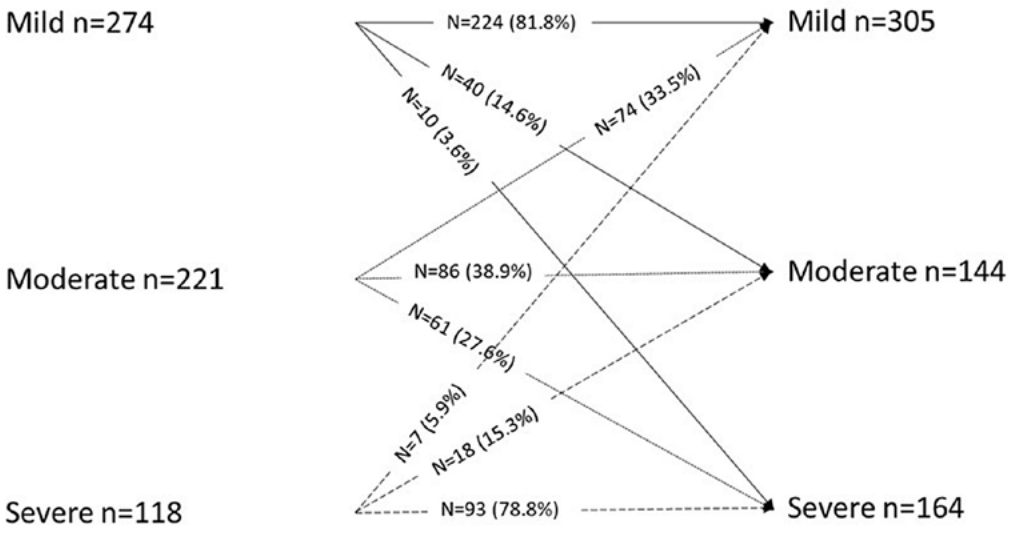

Figure 1. Changes in MR severity from baseline until the end-of follow-up

Presentation time
10.30-10.40

Riku Kiviluoto, MSc
University of Eastern Finland

Rotating frame spin-lock cardiac magnetic resonance imaging method can distinguish diffuse myocardial fibrosis in heart failure with preserved ejection fraction in mice at 9.4 T

Riku Kiviluoto, University of Eastern Finland; Diana Törmä, University of Eastern Finland; Ahmed Tawfek, University of Eastern Finland; Aleksi Leikas, University of Eastern Finland; Eetu Räihä, University of Eastern Finland; Mari Merentie, Heart Hospital Nova; Anna-Kaisa Ruotsalainen, University of Eastern Finland; Elias Ylä-Herttuala, University of Eastern Finland; Seppo Ylä-Herttuala, University of Eastern Finland

Aim

Incidence and prevalence of heart failure with preserved ejection fraction (HFpEF) continue to rise globally, and current imaging methods, including echocardiography and cardiac magnetic resonance imaging (CMRI) methods, are insufficient to provide accurate characterisation of diffuse fibrosis. This study aimed to investigate the capabilities of rotating frame spin-lock continuous-wave T1r (CWT1r) and relaxation along a fictitious field with rank 2 (RAFF2) CMRI methods, complementary to conventional T1 and late gadolinium enhancement (LGE) for imaging myocardial diffuse fibrosis in early HFpEF.

Methods

HFpEF was induced with s.c. angiotensin II infusion for 28 days, and sham-operated mice were used as controls. Echocardiography imaging was performed to assess the progression of HFpEF on days 0, 14 and 28. CMRI with conventional T1 and LGE methods were compared with rotating frame spin-lock CWT1r and RAFF2 methods, performed on days 14 and 28 of the experiment. Remote and fibrotic areas were delineated on the CMRI relaxation time maps and compared with corresponding areas in histological picrosirius red -stained cardiac sections.

Results

Rotating frame relaxation time maps revealed global diffuse fibrosis in HFpEF mice (Figure 1). Early myocardial diffuse fibrosis was distinguishable by day 14, and fibrotic remodelling in the left ventricle in HFpEF group was visible with RAFF2 at days 14 and 28 (Figure 2B). CWT1r also showed an increasing trend in relaxation time constant values on day 14, and CWT1r showed elevated relaxation time constants on day 28 in the HFpEF group (Figure 2A). In comparison, conventional T1 showed increased relaxation time values only on day 28, whereas LGE did not show any contrast agent accumulation in the myocardium (Figure 1 C-D). Histology supported our CMRI findings (Figure 1 A-C, E).

Conclusions

Rotating frame spin-lock CWT1r and RAFF2 CMRI methods are more sensitive to characterise myocardial diffuse fibrosis than conventional T1 and LGE methods in progressing HFpEF in mice, suggesting that the rotating frame spin-lock methods have the potential to distinguish myocardial collagen deposition, creating endogenous contrast, without the use of intravenously administered contrast agents and with reduced total scan time.

Presentation time
10.30-10.40

Riku Kiviluoto, MSc
University of Eastern Finland

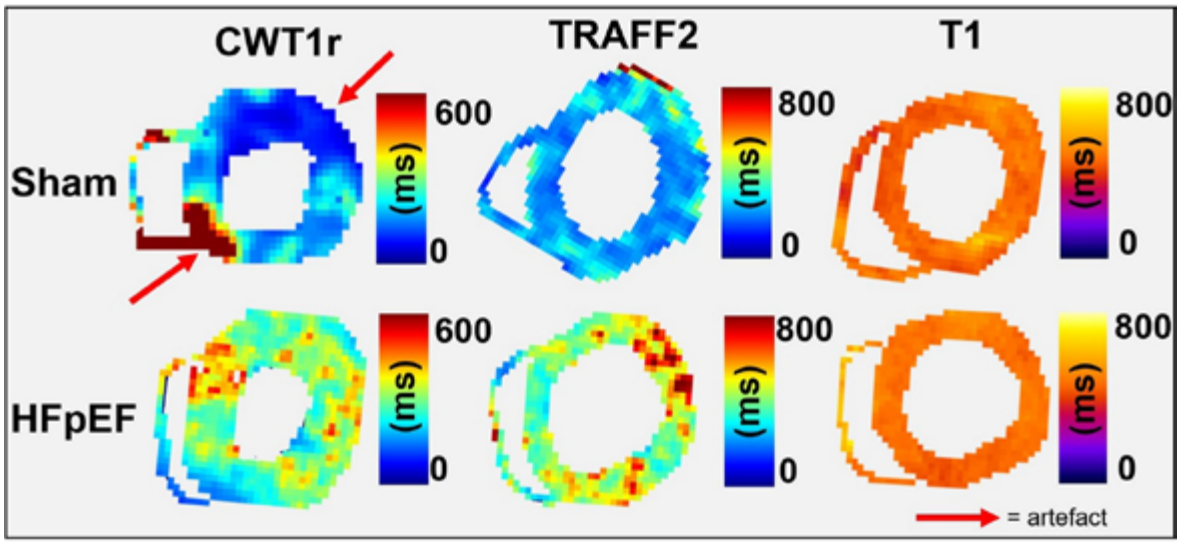

Figure 1. Representative rotating frame and conventional relaxation time maps of sham (upper row) and HFpEF (lower row) mouse. HFpEF, heart failure with preserved ejection fraction; CWT1r, Continuous wave T1r; RAFF2, Relaxation along a fictitious field with rank 2.

Presentation time
10.30-10.40

Riku Kiviluoto, MSc
University of Eastern Finland

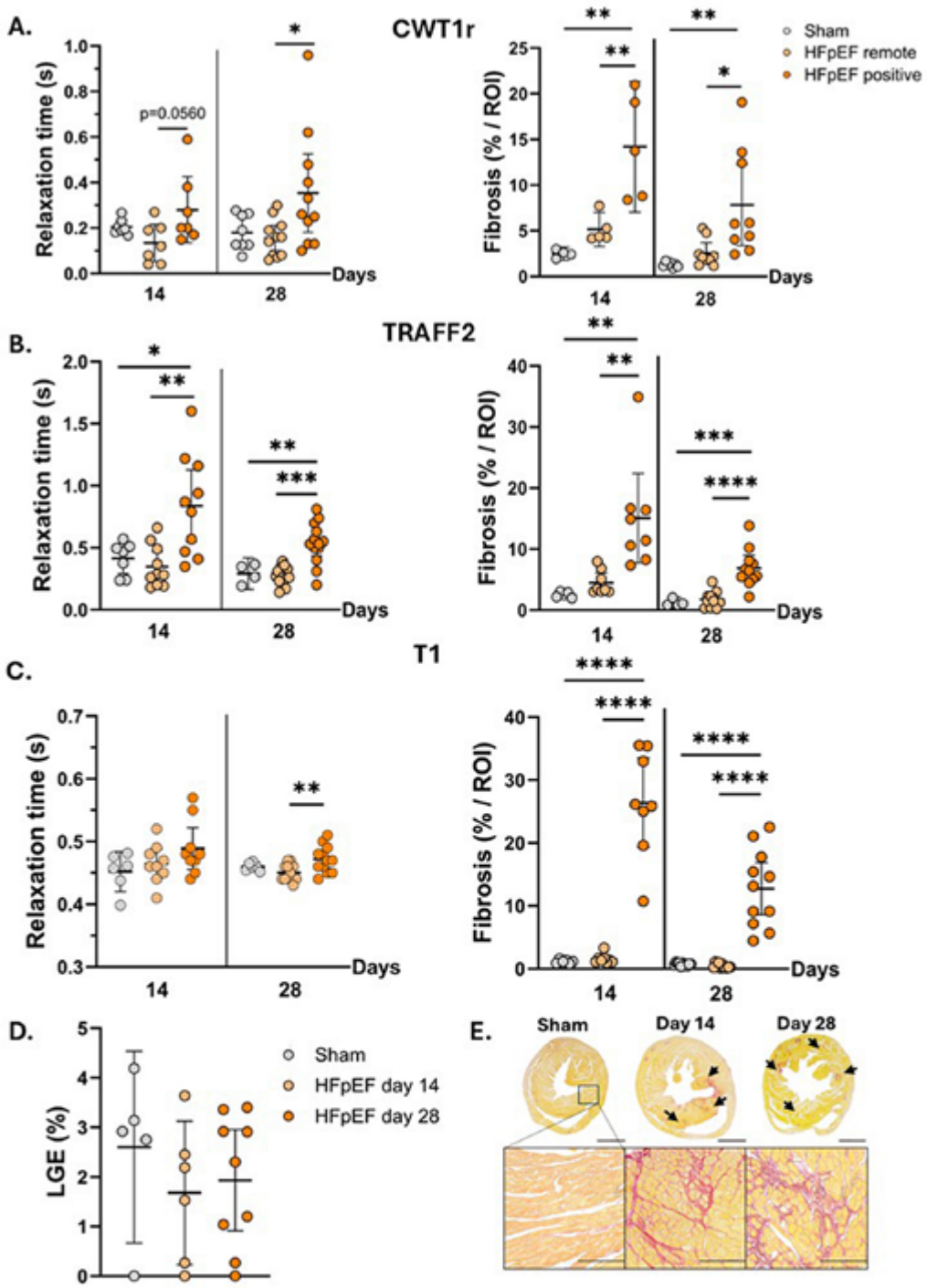

Figure 2. A-C: CWT1r, TRAFF2 and T1 relaxation times from sham, HFpEF remote and HFpEF positive regions of interest and the corresponding fibrosis depositions. D: Late gadolinium enhancement (LGE) accumulation in the myocardium. E: Representative histological Picrosirius red –stained cardiac sections. Data presented as mean with 95% CI (Statistical analysis was performed using one-way ANOVA followed by Tukey's post-hoc test (*p<0.05; **p<0.01; ***p<0.001; ****p<0.0001). CWT1r, Continuous wave T1r; RAFF2, Relaxation along a fictitious field with rank 2; HFpEF, heart failure with preserved ejection fraction;

Presentation time
10.40-10.50

Eero Jalli, MD
Satasairaala

Does the association between oral anticoagulation and stroke risk differ by CHA_2DS_2-VA score in patients with atrial fibrillation? A nationwide cohort study

Eero Jalli, Satasairaala; Lauri Leppiniemi, University of Turku; Jussi Jaakkola, Satasairaala; Ville Langén, Turku University Hospital; Juhani Airaksinen, Turku University Hospital; Olli Halminen, University of Eastern Finland; Jukka Putaala, Helsinki University Hospital; Pirjo Mustonen, University of Turku; Jari Haukka, University of Helsinki; Juha Hartikainen, Kuopio University Hospital; Miika Linna, University of Eastern Finland; Mika Lehto, Helsinki University Hospital; Konsta Teppo, University of Turku

Aim

Oral anticoagulation (OAC) therapy has been shown to reduce stroke risk by approximately two-thirds in patients with atrial fibrillation (AF) with high stroke risk. In contrast, recent studies in patients with subclinical, device-detected AF and lower baseline stroke risk have reported only a one-third reduction with direct oral anticoagulants (DOAC). Data on the effects of OAC therapy in patients with clinical AF and lower stroke risk are limited, and it remains unclear whether the benefit of OAC therapy is consistent across different stroke risk profiles in patients with clinical AF. Therefore, we conducted a nationwide retrospective cohort study to evaluate whether the magnitude of stroke risk reduction associated with OAC therapy varies according to baseline stroke risk as defined by the CHA_2DS_2 VA score.

Methods

The Finnish AntiCoagulation in Atrial Fibrillation (FinACAF) study includes all patients with AF in Finland between 2007 and 2018. Data were obtained from national registries covering all levels of care. Incidence and incidence rate ratio (IRR) of ischemic stroke were calculated for follow-up periods with and without OAC therapy, defined in a time-dependent manner.

Results

We identified 210 434 patients with new-onset AF and a CHA_2DS_2-VA score ≥ 1. The crude stroke rates increased as the CHA_2DS_2 VA score rose from 1 to 8, both with and without OAC therapy (0.79 to 3.65 and 0.90 to 7.78 per 100 patient years, respectively). OAC therapy was associated with a lower stroke rate across the CHA_2DS_2-VA score spectrum, with the association increasing gradually from approximately a 25% reduction among patients with CHA_2DS_2-VA score 1 and then stabilizing at approximately a 60% reduction among patients with CHA_2DS_2-VA ≥ 3. The pattern was similar for DOACs and vitamin K antagonists (VKAs), but the reduction in stroke rate with VKAs was smaller than that observed with DOACs across the studied CHA_2DS_2-VA score spectrum. Adjusted ten-year number needed to treat values were 45.3 and 9.7 for CHA_2DS_2-VA scores 1 and 2, respectively, and then plateaued at approximately 3 for higher risk scores.

Conclusions

In patients with AF, OAC therapy is associated with a reduced risk of stroke across CHA_2DS_2 VA scores from 1 to 8. However, the relative effect varies and is smaller among those with lower stroke risk scores, highlighting the importance of individualized stroke risk assessment, particularly among patients with lower baseline stroke risk.

Presentation time
10.40-10.50

Eero Jalli, MD
Satasairaala

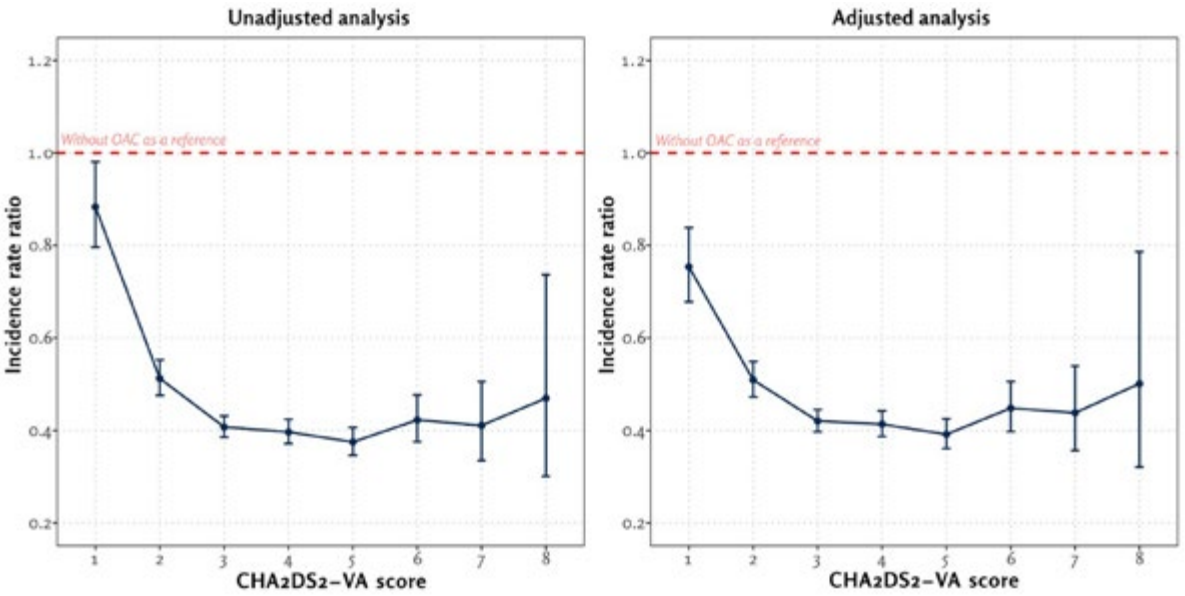

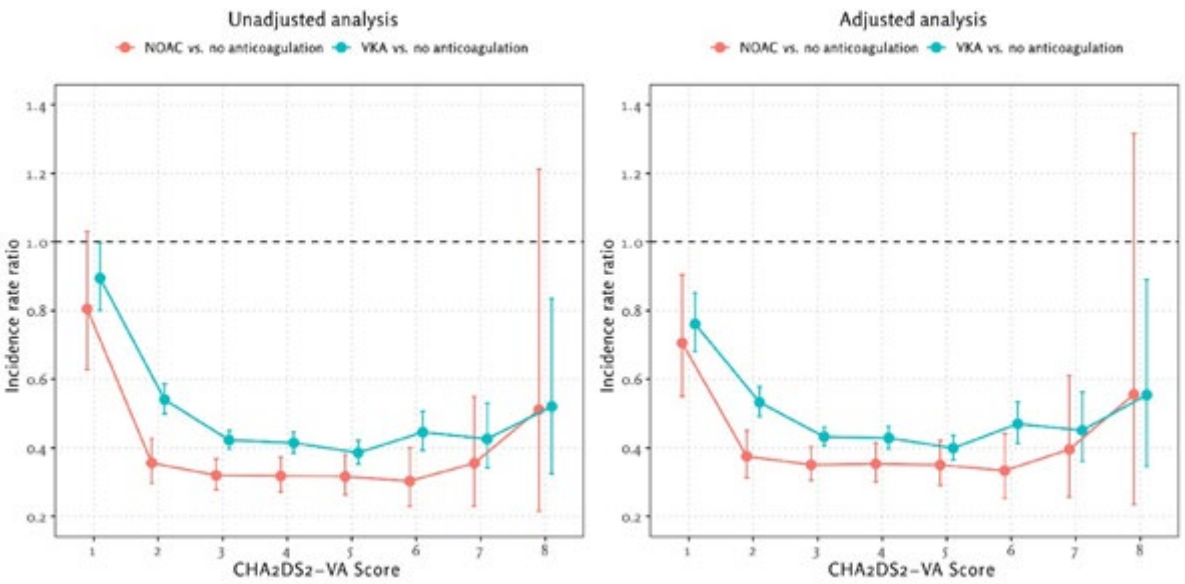

Presentation time
10.50-11.00

Lotta Poltto, Master of Science
HUS Helsinki University Hospital

Next-generation sudden cardiac death risk assessment in hypertrophic cardiomyopathy: integrating cardiac magnetic resonance imaging with artificial intelligence

Lotta Poltto, HUS Helsinki University Hospital; Tiina Ojala, HUS Helsinki University Hospital; Juha Peltonen, HUS Helsinki University Hospital; Annamaria Mustonen, HUS Helsinki University Hospital; Tiina Heliö, HUS Helsinki University Hospital; Teemu Vepsäläinen, HUS Helsinki University Hospital; Tekla Hiirsalmi, HUS Helsinki University Hospital; Minna Mecklin, Tampere University Hospital; Aino Keskinen, HUS Helsinki University Hospital; Lauri Lehmonen, HUS Helsinki University Hospital

Aim

Hypertrophic cardiomyopathy (HCM) is a major cause of sudden cardiac death (SCD), yet current stratification—based on HCM Risk-SCD scores combining echocardiographic, clinical, and familial data—has important limitations. Cardiac magnetic resonance (CMR) offers superior tissue characterization and may improve risk prediction. We evaluated whether an artificial intelligence (AI) regression model using CMR-derived features can enhance the accuracy and reproducibility of SCD-risk assessment.

Methods

Our retrospective cohort included 437 genetically confirmed sarcomere-positive patients, of whom 261/298 underwent 1.5T CMR (3T studies excluded). The 5-year ESC Risk of SCD was calculated using ESC recommended algorithms. CMR acquisition included cine short-axis and four-chamber views, left ventricle T1 mapping, and late gadolinium enhancement. An automated pipeline standardized all images and performed data augmentation. Processed datasets were then used to train a DenseNet-based convolutional neural network (90% training split), with the ESC HCM Risk-SCD score as the regression target.

Results

The AI model predicted HCM Risk-SCD values with a mean absolute error below 2 in the validation dataset. All combinations of CMR sequence inputs were evaluated. Models including cine images consistently produced the most accurate and stable predictions. Adding other CMR modalities to cine data further reduced prediction error.

Conclusions

The CNN-based AI model accurately predicted the HCM Risk-SCD index from CMR images, demonstrating the potential of CMR as a robust tool for SCD-risk assessment in HCM. As the dataset includes patients with documented cardiac SCD events, the next step is to train and evaluate the model directly against observed SCD outcomes to estimate absolute risk. Future work will also require external validation in independent cohorts to confirm model performance and generalizability.

Presentation time
11.00-11.10

Samu Saarimäki, Master of Science
University of Oulu

Combined targeting of AT1 and CTGF for heart failure therapy

Samu Saarimäki, University of Oulu; Zoltan Szabo, University of Oulu; Sini Skarp, University of Oulu; Ruizhu Lin, University of Oulu; Johanna Magga, University of Oulu; Risto Kerkelä, University of Oulu

Aim

Renin-angiotensin-aldosterone system (RAAS) is an important driver of myocardial growth and remodeling and a key target of guideline-directed heart failure therapy. Connective tissue growth factor (CTGF) regulates extracellular matrix homeostasis and development of myocardial fibrosis and heart failure. In the present study, we investigated therapeutic potential of combined targeting of CTGF and angiotensin II type 1 receptor (AT1) on development of myocardial fibrosis and heart failure.

Methods

Male C57BL6 mice were subjected to thoracic aortic constriction (TAC) model for 2 or 8 weeks to induce pressure overload. After inducing TAC, mice were treated either with CTGF neutralizing monoclonal antibody (CTGF mAb) plus AT1-receptor blocker losartan, control IgG plus losartan, or control IgG alone for the duration of the study. Cardiac structure and function were assessed by echocardiography and myocardial fibrosis, and hypertrophy were evaluated by histological staining of cardiac FFPE sections using Picrosirius Red (PSR) and Wheat Germ Agglutinin (WGA), respectively. Left ventricular (LV) gene expression was analyzed by qPCR, RNA sequencing, and pathway enrichment analysis (IPA).

Results

Two weeks of TAC induced an increase in LV posterior wall thickness and increased heart weight, but no difference was observed between treatment groups. qPCR analysis showed that targeting CTGF and AT1 but not AT1 targeting alone attenuated the TAC-induced increase in LV expression of Nppa, Ccn2 and Acta1. Echocardiography analysis at 8 weeks after TAC showed that combined targeting of CTGF and AT1 but not AT1 targeting only preserved LV ejection fraction and attenuated the TAC-induced increase in LV mass. PSR staining showed a trend toward reduced fibrosis in the losartan-treated groups, while WGA staining indicated a similar trend towards decreased average cardiomyocyte cell size. RNA sequencing analysis of LV samples collected 8 weeks after TAC identified 339 transcripts differentially expressed between CTGF mAb plus losartan vs control IgG plus losartan groups. Ingenuity pathway enrichment analysis of the RNA-sequencing data showed that the combined CTGF/ AT1 targeting reduced the activation of genes related to organization of extracellular matrix, dilated cardiomyopathy signaling, and reduced expression of NFAT regulatory genes.

Conclusions

These findings suggest that combined inhibition of CTGF and AT1 provides additive benefit compared to AT1 inhibition alone in attenuating the development of hemodynamic pressure overload induced heart failure.

Presentation time
11.10-11.20

Olli Rantula, MD, MSc
University of Eastern Finland

A Deep Neural Network for Interpreting Wearable ECG Data in Atrial Fibrillation

Olli Rantula, University of Eastern Finland; Jukka Lipponen, University of Eastern Finland; Jari Halonen, University of Eastern Finland; Helena Jäntti, North Karelia Central Hospital; Tuomas Rissanen, University of Eastern Finland; Mika Tarvainen, University of Eastern Finland; Noora Naukkarinen, University of Eastern Finland; Eemu-Samuli Väliaho, University of Helsinki; Onni Santala, Kuopio University Hospital; Jagdeep Sedha, University of Eastern Finland; Tero Martikainen, Kuopio University Hospital; Juha Hartikainen, University of Eastern Finland

Aim

Atrial fibrillation (AF) and atrial flutter (AFL) are common arrhythmias associated with risk of ischemic stroke, which can be reduced with anticoagulation therapy. Thus, early diagnosis of AF and AFL is essential. However, diagnosis may be challenging due to the paroxysmal and asymptomatic nature of these arrhythmias.

Current diagnostic workflows involve time-consuming and resource-intensive manual review of noisy signals and prolonged recordings. We evaluated a mobile system combining wireless wearable single-lead chest strap electrocardiogram (ECG) and novel deep neural network (DNN) based artificial intelligence (AI) method for detecting AF/AFL episodes, AF/AFL burden, and rhythm change and the detection delay in the change from AF/AFL to sinus rhythm (SR). Rhythm classification performance was also assessed.

Methods

A total of 116 patients with recent-onset AF or AFL undergoing cardioversion were monitored using a mobile single-lead chest strap ECG system. Simultaneously, a three-lead Holter ECG served as the reference. The DNN-based AI analyzed single-lead chest strap ECG data to detect AF/AFL, non-AF/AFL rhythm, and non-interpretable segments, as well as to estimate AF/AFL burden and detect rhythm change. Performance metrics included sensitivity, specificity, PPV, NPV and the intraclass correlation coefficient (ICC) for AF and AFL burden estimation.

The sensitivity and specificity for detecting AF/AFL were 91.9% and 99.6%, respectively. The sensitivity for detecting AF was 96.2%, whereas for AFL it was 55.8%. The PPV and NPV for AF/AFL detection were 99.5% and 93.1%, respectively. The ICC between AF/AFL burden estimated by the DNN-based AI method and that derived from physician-interpreted reference ECG was 0.96 (95% CI: 0.94–0.97; P<.001). Rhythm change detection occurred within one minute in most cases.

Conclusions

The mobile single-lead chest strap ECG system powered by a DNN-based AI algorithm demonstrated strong performance in detecting AF, estimating AF burden, and recognizing rhythm change to SR. This AI-driven approach enables automated and accurate rhythm analysis, supporting clinical decision-making. Further validation in real-world ambulatory settings is warranted.

Presentation time
11.20-11.30

Essi Pirskanen, Medical Student
Tampere University Heart Hospital and Tampere University

The presence of cysts suggests for degenerative acute type A aortic dissection

Essi Pirskanen, Tampere University Heart Hospital and Tampere University; Ivana Kholova, Tampere University Hospital and Tampere University, Fimlab Laboratories; Timo Paavonen, Tampere University Hospital and Tampere University, Fimlab Laboratories; Ari Mennander, Tampere University Heart Hospital and Tampere University

Aim

Acute type A aortic dissection (ATAAD) is characterized by aortic wall degeneration. Aortic wall degeneration, including cystic media necrosis, may share pathogenetic similarities with cyst development. We investigated whether the presence of ovarian, liver, epididymal, and/or renal cysts is associated with ascending aortic wall degeneration in patients with ATAAD.

Methods

A total of 120 consecutive patients who underwent surgery for ATAAD at Tampere University Heart Hospital were evaluated. Ascending aortic wall tissue resected during surgery underwent histological assessment for 11 variables indicative of degeneration. Patients were divided into two groups according to the presence of cysts to those with and those without cysts (n=45 and n=75). These two groups were compared during a mean 6.7-year (standard deviation [SD] = 4.6) follow-up.

Results

The mean age for all patients was 66 years (SD 12). Chronic obstructive pulmonary disease was more frequent in patients with cysts versus not (31.1% versus 12.0%, P=0.016, respectively). Biological conduit prosthesis was used more frequently among patients with cysts as compared with those without (44.4% versus 17.3%, P=0.003), whereas an aortic root-sparing operation was less frequently performed on patients with cysts versus without cysts (40.0% versus 62.7%, P=0.023). Histopathological analysis demonstrated severe elastic fiber thinning (1.3 ± 0.8 vs. 0.9 ± 0.9, P=0.020, respectively) and increased presence of vasa vasorum thickening (26.7% vs. 12.0%, P=0.049, respectively) in patients with cysts vs. without. There were 54 deaths, with no statistically significant difference between the groups (log-rank P=0.910). However, multivariable Cox regression analysis adjusted for age and sex showed a higher risk for aortic reoperations in patients with cysts (odds ratio: 1.050, 95% confidence interval: 1.015-8.044, P=0.047).

Conclusions

Histopathological findings of the ascending aorta during ATAAD reveal an increased extent of elastic fiber thinning and presence of vasa vasorum thickening in patients with cysts vs. without. Patients with cysts exhibit a distinctive pattern of aortic wall degeneration associated with ATAAD often requiring a conduit prosthesis replacing the aortic root together with the ascending aorta.

Presentation time
11.20-11.30

Essi Pirskanen, Medical Student
Tampere University Heart Hospital and Tampere University

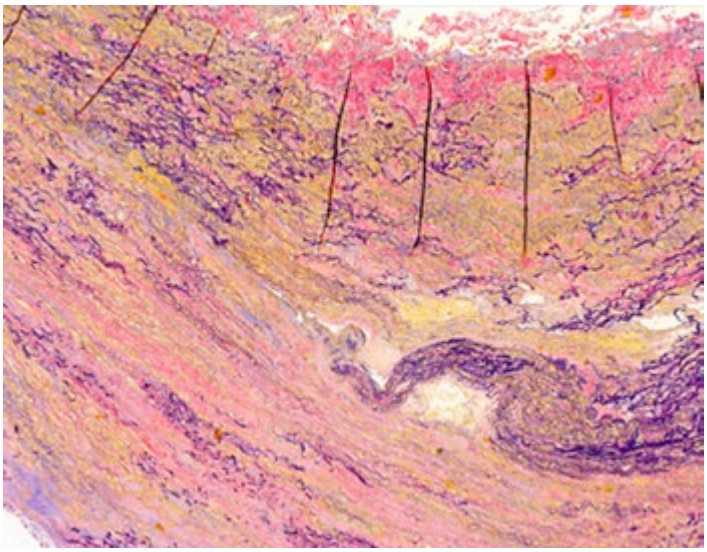

Table 1. Histopathology

		All (n=120)	With cysts (n=45)	Without cysts (n=75)	*P*-value
Mucoid Extracellular Matrix Accumulation, n		120 (100.0%)	45 (100.0%)	75 (100.0%)	>0.999
	Lamellar, mean (SD)	1.44 (0.499)	1.49 (0.506)	1.41 (0.496)	0.422
	Extent, mean (SD)	1.99 (0.330)	2.02 (0.336)	1.97 (0.328)	0.433
Elastic Fiber Thinning, n		76 (63.3%)	34 (75.6%)	42 (56.0%)	0.034
	Extent, mean (SD)	1.07 (0.905)	1.31 (0.848)	0.92 (0.912)	0.020
	Severity, mean (SD)	0.93 (0.837)	1.07 (0.780)	0.85 (0.865)	0.151
Elastic Fiber Disorganization, n		98 (81.7%)	39 (86.7%)	59 (78.7%)	0.335
	Extent, mean (SD)	1.35 (0.816)	1.42 (0.753)	1.31 (0.854)	0.472
Smooth Muscle Cell Nuclei Loss, n		103 (85.8%)	36 (80.0%)	67 (89.3%)	0.182
	Type, mean (SD)	1.37 (0.721)	1.18 (0.747)	1.48 (0.685)	0.023
	Extent, mean (SD) (rare)	1.59 (0.893)	1.47 (0.944)	1.67 (0.859)	0.281
Medial fibrosis, n		15 (12.5%)	5 (11.1%)	10 (13.3%)	0.784
Vaso vasorum medial thickening, n		21 (17.5%)	12 (26.7%)	9 (12.0%)	0.049
Adventitial fibrosis, n		22 (18.3%)	6 (13.3%)	16 (21.3%)	0.335

n=number of cases, SD=standard deviation

Presentation time
11.30-11.40

Yi Li, PhD Candidate
University of Oulu

Non-invasive imaging of the sinoatrial node structure using quantitative MRI: from histology-validated ex vivo porcine study to first human in vivo assessment

Yi Li, University of Oulu; Victor Casula, University of Oulu; Timo Liimatainen, University of Oulu

Aim

The sinoatrial node (SAN) is the primary cardiac pacemaker, but its 3D structure is difficult to assess non-invasively. This study explored the potential of quantitative MRI for SAN imaging by combining histology-validated ex vivo porcine experiments with preliminary human in vivo data. Linking ex vivo validation with in vivo feasibility, we aimed to provide insights into the structure of SAN and translational potential.

Methods

Ex vivo porcine heart samples (n=7) were scanned on a 3T clinical MRI system to acquire quantitative relaxation time maps (T1ρ, TRAFF2, T1, T2) for SAN characterization, with Masson's Trichrome histology validating localization. Five human subjects (three patients without known SAN dysfunction and two healthy volunteers) underwent cardiac MRI at 1.5 T using ECG-gated, breath-hold acquisitions, including native T1, T2, T1ρ mapping and late gadolinium enhancement (LGE) imaging. Regions of interest (ROI) were defined in the SAN region based on anatomical landmarks and LGE guidance, with remote right atrial myocardium as reference. Tissue contrast was quantified using relative relaxation time differences (RRTD), and statistical comparisons were performed using paired two-tailed t-tests for both ex vivo and in vivo data.

Results

Ex vivo T1ρ mapping clearly distinguished the SAN from surrounding atrial myocardium (Figure 1A–B). Segmented SAN areas from T1ρ maps strongly correlated with histology-defined regions (Figure 1C), validating anatomical localization. 3D reconstruction highlighted the spatial organization of the SAN within the ex vivo heart (Figure 1D). Quantitative MRI consistently showed significant higher relaxation times in the SAN compared with remote myocardium across all measured parameters, with T1ρ and TRAFF providing the highest contrast (Figure 1E). In vivo LGE-CMR identified of the SAN at the junction of the superior vena cava and right atrium, adjacent to the crista terminalis (Figure 2A). Quantitative MRI maps, including T1ρ, T1, and T2, highlighted the SAN region with higher relaxation times relative to surrounding myocardium (Figure 2B–D). Relative relaxation time differences (RRTD) confirmed clear tissue contrast, with T1ρ and T2 providing the most pronounced distinction (Figure 2E).

Conclusions

Combined ex vivo and in vivo quantitative MRI enables clear SAN visualization and characterization. Ex vivo mapping validated anatomical localization and 3D structure, while in vivo imaging showed that the SAN can be non-invasively distinguished from surrounding atrial myocardium. T1ρ and T2 provided the highest tissue contrast, highlighting the potential of quantitative MRI for translational assessment of SAN structure and function in humans.

Presentation time
11.30-11.40

Yi Li, PhD Candidate
University of Oulu

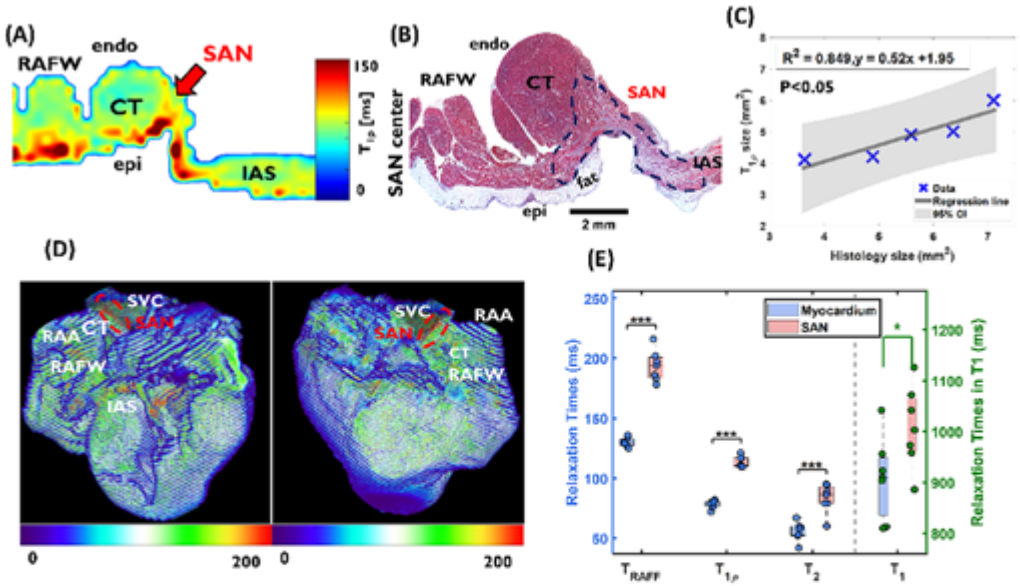

Figure 1. Ex vivo imaging of the sinoatrial node using quantitative MRI.
(A) $T_{1\rho}$ relaxation time map showing contrast between the SAN and atrial myocardium. (B) Masson's trichrome histology of the sinoatrial node. (C) Linear correlation of sinoatrial node areas segmented by $T_{1\rho}$ mapping and histology. (D) 3D reconstruction of the sinoatrial node from $T_{1\rho}$ mapping. (E) Quantitative MRI relaxation times of the SAN and atrial myocardium.
CT, crista terminals; IAS, interatrial septum; RAA, right atrial appendages; RAFW, right atrial free wall; SVC, superior vena cava; SAN, sinoatrial node.
Adapted from the figures of Li et al. Rotating frame relaxation time mapping for the visualization of the sinoatrial node without contrast agent. NMR Biomed, 2025 (under CC BY license)

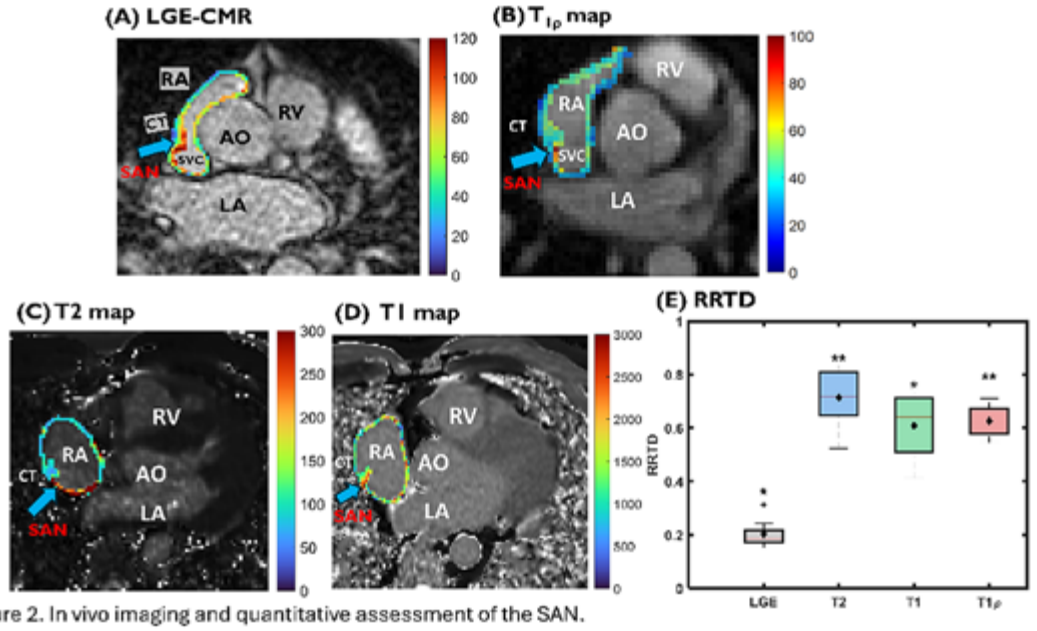

Figure 2. In vivo imaging and quantitative assessment of the SAN.
(A) LGE-CMR showing the SAN (blue arrows) at the junction of the superior vena cava (SVC) and right atrium (RA), adjacent to the crista terminalis (CT).
(B) In vivo $T_{1\rho}$ map of SAN region (higher relaxation time)
(C) Native T1 map and (D) T2 map acquired from the same subject.
(E) Relative relaxation time difference (RRTD) between the SAN and remote myocardium for each quantitative MRI parameter (*P < 0.05, **P < 0.01).
AO, aorta; CT, crista terminals; LA, left atrium; RA, right atrium; RV, right ventricle; SVC, superior vena cava; SAN, sinoatrial node.

Presentation time
11.40-11.50

Ansa Hakala, Bachelor of Medicine
University of Eastern Finland

Association between aortic length and 4D flow parameters: wall shear stress and flow displacement

Ansa Hakala, University of Eastern Finland; Heta Rasinkangas, University of Eastern Finland; Johanna Laakkonen, University of Eastern Finland; Petri Saari, Kuopio University Hospital; Marja Hedman, Kuopio University Hospital and University of Eastern Finland; Saara Sillanmäki, Kuopio University Hospital and University of Eastern Finland

Aims
Ascending aortic diameter is traditionally used to guide clinical decision-making in patients with thoracic aortic dilatation; however, ascending aortic length (AAL) has recently emerged as an additional risk marker for adverse aortic events. The aim of this study was to investigate the association between ascending aortic length and aortic hemodynamics assessed by four-dimensional flow magnetic resonance imaging (4D flow MRI), focusing on wall shear stress (WSS) and flow displacement (FD).

Methods
This retrospective study included 59 patients undergoing preoperative 4D flow MRI prior to ascending aortic graft surgery for aortic dilatation. Ascending aortic length and aortic diameters were measured from anatomical MRI. Hemodynamic parameters, including maximal, axial, and circumferential WSS as well as FD, were quantified at predefined planes along the thoracic aorta. Patients were stratified according to AAL (≥11 cm vs. <11 cm) and valve morphology (bicuspid vs. tricuspid aortic valve). Associations between hemodynamic parameters, AAL, blood pressure, and clinical characteristics were analyzed.

Results
Patients with an AAL ≥11 cm demonstrated significantly higher WSS and FD compared with patients with shorter ascending aortas. These hemodynamic alterations were more evident in patients with bicuspid aortic valve than in those with tricuspid valves. Ascending aortic length, adjusted for valve type and sex, was positively associated with mid-tubular FD. In contrast, WSS was associated with systolic blood pressure at the aortic root, independent of valve type. Age, height, and weight showed no significant associations with WSS or FD.

Conclusions
Increased ascending aortic length is associated with altered aortic hemodynamics, particularly elevated WSS and FD, with more pronounced changes observed in patients with bicuspid aortic valve. These findings suggest that ascending aortic length may provide complementary information for assessment in patients with aortic dilatation.

Meeting is supported by unrestricted educational grant from Boehringer Ingelheim.